The evolution of the transport coefficients for the transient process after the ECRH switch-on/off in the T-10 tokamak

V.F. Andreev, A.V. Danilov, Yu.N. Dnestrovskij, M.V. Ossipenko,
K.A. Razumova, A.V. Sushkov

Nuclear Fusion Institute, RRC "Kurchatov Institute", 123182, Kurchatov Sq.1, Moscow, Russia

e-mail contact of main author: andreev@fusion.ru

Abstract. The study of the transient process after the ECRH switch-on/off in the T-10 tokamak shows that the electron ITB appears nearby the resonance surface q~3/2 in regimes with the suppressed saw-tooth oscillations. When the gradient of the electron temperature in the plasma centre after the additional on-axis ECR heating exceeds some critical value the electron ITB is destroyed and the heat flux spreads from the heating region to the plasma periphery practically instantly. It looks like a jump of the heat flux through the all plasma region. Therefore to describe the electron heat transport in tokamak plasma after the ECRH switch-on/off three different physical processes should be taken into account: a) the transient process of plasma heating inside the region bounded by the temporal electron ITB; b) the electron ITB destruction accompanied by the heat efflux to the plasma periphery during the hundreds of microseconds; c) the consequent diffusive evolution of the electron temperature profile with the conservation of the relative electron temperature gradient $\nabla T/T$.

1. Introduction

Transient electron heat transport analysis allows us to study the response of the heat transport due to external disturbance and to reconstruct the transport coefficients as a function of plasma parameters. In particular the analysis of the transient process after the electron cyclotron resonance heating (ECRH) switch-on/off is very attractive to understand the electron heat transport.

The ECRH of tokamak plasma has two useful peculiarities. The first is the well-localised power absorption region under the microwave launch perpendicular to the magnetic field. The half-width of the ECRH power deposition function is typically 2÷4 cm. The second is the fast change of the ECRH power after the gyrotrons switch-on/off. As example in T-10 tokamak the characteristic time of the nominal ECRH power achievement is less than 150÷200 μs, when the gyrotron is fed from the bank of capacitors, (power supply system “Beton”). Duration of the ECRH power switch-off is even faster – about 50 μs.

Regimes with suppressed saw-tooth were analyzed in [1-4] for tokamaks T-10 and TEXTOR. In such regimes the influence of the electron ITB on the improvement of the confinement was revealed. In T-10 it was shown, that after the off-axis ECRH switch-off, zone of the improved confinement appears in the core plasma [4-5]. The central electron temperature started to decrease with the time delay about τ~20 мс after the off-axis ECRH switch-off. The similar experiment in TEXTOR shows the time delay of the decrease of the central temperature about τ~35 мс [3-4] after the off-axis ECRH switch-off.

The confinement improvement in transient process after the off-axis ECRH switch-off was explained by the appearance of the electron ITB around a point ρ~0.2÷0.3 ($\rho=r/a$) [1-4]. The condition of the electron ITB formation was analyzed in these works in details.

It is well known that in tokamak plasma with auxiliary heating the electron temperature profile evolves selfconsistently. This property is known as “profile resilience” or “profile stiffness” [5-11]. The empirical model based on the strong increase of the electron heat diffusivity when the electron temperature profile T_e exceeds a threshold value of ∇T or $\nabla T/T$ is

used for the description of such profile behavior [12-15]. From the theoretical point of view the two possible sources of turbulent transport can cause such a dependence: the Trapped Electron Modes (TEM) coupled with the Ion Temperature Gradient (ITG) modes and the Electron Temperature Gradient (ETG) modes.

The minimum of the free plasma energy functional gives also the basis for the interpretation of the experiment [16].

In our previous papers [17-18] the analysis of the transient process after the ECRH switch-on/off was done by careful interpretation of the experimental data based on the inverse problem method. It was shown, that the adequate description of the transient process demands the introduction of jump of transport coefficients after the ECRH switch-on/off through all plasma cross section. It means that the electron temperature at the periphery must change simultaneously. Therefore these results indicate to non-local electron transport at the transient process after the ECRH switch-on/off [17-18].

The different physical mechanisms can be proposed to explain the fast jump of the heat flux. Probably the plasma reacts to the ECRH power input directly. This can happen due to partial destruction of magnetic surfaces after the increase of deposited power. The other possibility is the fast propagation of information through the turbulent cell chains, and, as a result, the change of critical gradients over the plasma cross-section.

In this paper we study the existence of the electron ITB at the steady state in the regime with suppressed saw-tooth oscillations and analyze the response of the electron heat transport to the ECRH switch-on/off in the T-10 tokamak.

2. The ECRH experiments in T-10

The experimental data were obtained from the on- and off-axis ECRH discharges in T-10 (major radius R_0=150 cm, minor radius a=30 cm). The plasma current was I_P=185 kA, the toroidal magnetic field was close to B_Z=2.33 T, line averaged density changes in the range $\langle n\rangle \approx 1.4\times10^{19}/m^3$. The electron temperature is provided by the 18 channels ECE heterodyne radiometer with time resolution of 15 μs ($r=R-R_0$ – the coordinates of the measurement channel).

In order to increase the accuracy of the analysis the saw-tooth oscillations were suppressed by the off-axis ECRH (two gyrotrons with the frequency 140 GHz, and the total power P_{EC}~550 kW under the perpendicular microwave launch). For the chosen B_Z value the EC resonance for 140GHz takes place near $R_{EC}\approx R_0$-(12÷13 cm) at the high field side of tokamak plasma (dimensionless radius $\rho=r/a_0$=0.43÷0.46). After the saw-tooth oscillations suppression, the on-axis ECRH (shots #32916, #32917 - one gyrotron with the frequency 130 GHz, power P_{EC}~600 kW) and the off-axis ECRH (shot #32912, one gyrotron with the frequency 140 GHz, power P_{EC}~250 kW) were switched on/off.

Later on we will use the denotation $T_{SS}(r)$ for all pictures as the steady state electron temperature after the suppression of the saw-tooth oscillations by the off-axis gyrotrons.

Further in this work we will use the following definition of the electron ITB.

Definition. If the heat diffusivity coefficient χ^{TB} has the local minimum at the plasma radius r_{TB} then one can say that the electron ITB exists at this place.

3 The electron ITB with the suppressed saw-tooth oscillations

FIG.1 shows the sequence of time slices of the electron temperature profiles $T(r,t)$ after the on-axis ECRH switch-on with the suppressed saw-tooth oscillations (shot #32916). We see that the relative variation of the electron temperature is rigorously localized inside the zone – 6.30cm<r<+10.1cm

during time interval $\Delta t \approx 2.5$ ms. Note that the Shafranov's shift is nearly 2 cm. Therefore the size of this zone is equal to 8.2 cm if we will count from the magnetic axis (in relative units $\rho \sim 0.28$). Note that in Ohmic mode the phase inversion radius of the saw-tooth oscillations (the resonance surface $q \sim 1$) was equal to $\rho \sim 0.2$. So the calculations of the safety factor profile show that the value $\rho \sim 0.28 \div 0.35$ is close to the resonance surface $q \sim 3/2$ (shot #32916, ASTRA code).

FIG.2 shows the time evolution of the electron temperature $T(r,t)$ for the central channels of the measurement after the on-axis ECRH switch-on (shot #32916). We see that the temperature increases in the channel r=+10.1 cm just after the on-axis ECRH switch-on (the vertical solid line) but the temperature does not increase in the next channel r=+12.8 cm during the time interval $\tau_{TB} \sim 2.5$ ms (the vertical dashed line).

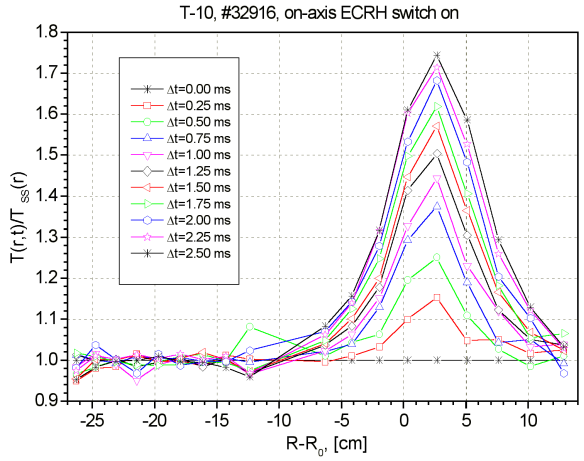

FIG.1. Time evolution of the relative electron temperature profile variation T(r,t) after the on-axis ECRH switch-on with the suppressed saw-tooth oscillations (shot #32916). Here R is the major radius, R_0 is the chamber centre, Δt is the time interval after the ECRH switch-on, $T_{SS}(r)$ is the steady state electron temperature before the ECRH switch-on.

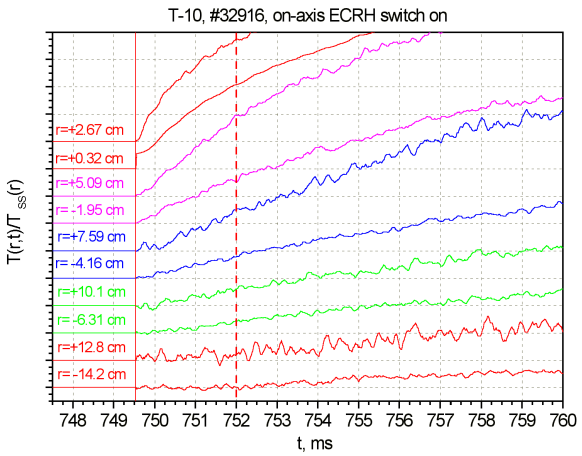

FIG.2. Time evolution of the temperature T(r,t) for the central channels -14.2 cm<r<+12.8 cm after the on-axis ECRH switch-on with the suppressed saw-tooth oscillations (shot #32916). Here $T_{SS}(r)$ is the steady state temperature before the ECRH switch-on. The vertical solid line is the moment of the switch-on. The vertical dashed line is the time delay of the temperature increase between channels r=+10.1 cm and r=+12.8 cm.

The heat diffusivity coefficient χ_e^{HPP} calculated from the temperature perturbation propagation between the channels r=+10.1 cm and r=+12.8 cm is equal to $\chi_e \sim 0.035$-0.10 m^2/s (the time interval 749.5-752 ms after the ECRH switch-on was considered).

FIG.3 shows the time evolution of the electron temperature for the central channels of the measurement after the off-axis ECRH switch-on (the third gyrotron 140 GHz, shot #32912) with the suppressed saw-tooth oscillations. One can see that the temperature increases in channel r=+10.2 cm just after the ECRH switch-on (the vertical solid line) but the temperature does not increase in the next channel r=+7.69 cm during the time interval $\tau_{TB} \sim 4.5$ ms (the vertical dashed line).

The heat diffusivity coefficient χ_e^{HPP} calculated from the temperature perturbation propagation between the channels r=+10.2 cm and r=+7.69 cm is equal to $\chi_e \sim 0.035$-0.10 m^2/s (the analysis was done for the time interval 800-804 ms after the ECRH switch-on). Similarly the heat diffusivity coefficient χ_e^{HPP} between the channels r=-6.22 cm and r=-4.07 cm is equal to $\chi_e \sim 0.03$-0.10 m^2/s.

FIG.4 shows the time evolution of the electron temperature for the central channels after the off-axis ECRH switch-off with the suppressed saw-tooth oscillations (the third gyrotron 140 GHz, shot #32912). We see that the temperature decreases in channel r=+10.2 cm just after the ECRH switch-off (the vertical solid line) but the temperature does not decrease in the next channel r=+7.69 cm during the duration τ_{TB}~4.5 ms (the vertical dashed line).

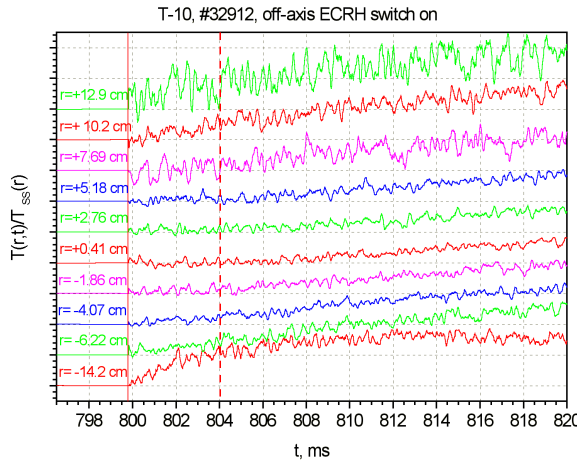

FIG.3. Time evolution of temperature for the central channels after the off-axis ECRH switch-on with suppressed saw-tooth oscillations (#32912). The vertical solid line is the moment of the ECRH switch-on. The vertical dashed line is the time delay of the temperature increase between channels r=+10.2 cm and r=+7.69 cm.

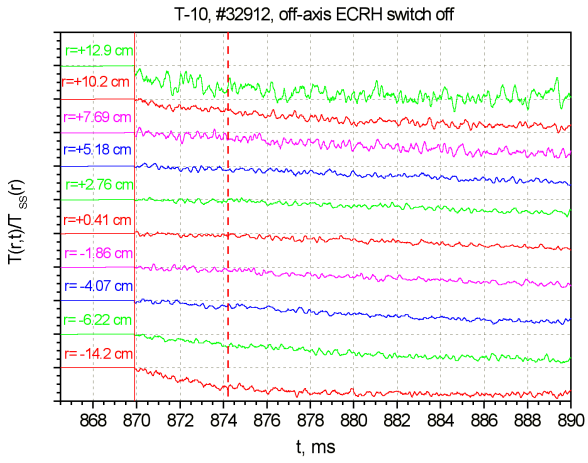

FIG.4. Time evolution of temperature for the central channels after the off-axis ECRH switch-off with the suppressed saw-tooth oscillations (#32912). The vertical solid line is the moment of the ECRH switch-off. The vertical dashed line is the time delay of the temperature decrease between channels r=+10.2 cm and r=+7.69 cm.

The heat diffusivity coefficient χ_e^{HPP} calculated from the temperature perturbation propagation between the channels r=+10.2 cm and r=+7.69 cm is equal to χ_e~0.04-0.11 m^2/s (the analysis was done for the time interval 4.5 ms after the ECRH switch-on). Similarly the heat diffusivity coefficient between channels r=-6.22 cm and r=-4.07 cm is equal to χ_e~0.03-0.1 m^2/s.

The Power Balance calculation (ASTRA code) gave the value of the heat diffusivity coefficient χ^{PB}~0.5÷0.6 m^2/s in the region ρ~0.28÷0.35 for the shot #32916 before the on-axis ECRH switch-on and for the shot #32912 before the off-axis ECRH switch-on/off (the saw-tooth oscillations were suppressed). At the same time the heat diffusivity coefficient calculated from the temperature perturbation propagation in this region is equal to χ_e~0.05-0.1 m^2/s.

Therefore there is the local minimum of the heat diffusivity coefficient in the region ρ~0.28÷0.35. The value of this local minimum χ^{TB} is 3÷4 times less then the average value of the heat diffusivity coefficient χ^{PB}. The size of this region is equal to Δ_{TB}~2.51 cm

So the analysis of the experimental data and the calculation of the heat diffusivity coefficient showed that the electron ITB appears in the region ρ~0.28÷0.35 (probably nearly the resonance surface q~3/2) after the suppression of the saw-tooth oscillations by off-axis ECRH.

4. The jump of the periphery heat flux

FIG.5 shows the time evolution of the electron temperature for the peripheral ECE channels after the on-axis ECRH switch-on with the suppressed saw-tooth oscillations (shot #32916). Note, that the temperature does not increase at peripheral channels at least during τ_{TB}~2.5 ms (the vertical dashed line). After this moment the temperature begins to increase in all channels practically simultaneously. The time delay could be on the level of Δt<0.5 ms.

FIG.6 shows the time evolution of the electron temperature for the peripheral channels of ECE after the on-axis ECRH switch-on with the suppressed saw-tooth oscillations (shot #32917, but with the input ECRH power is twice less than in shot #32916). Note, that the temperature does not increase in peripheral channels during τ_{TB}~5.0 ms (the vertical dashed line).

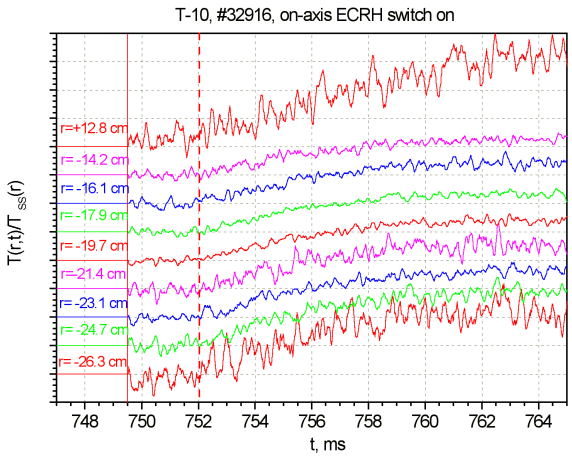

FIG.5. Time evolution of temperature for the peripheral channels 12.8 cm <|r|< 26.3 cm after the on-axis ECRH switch-on with the suppressed saw-tooth oscillations (shot #32916). $T_{SS}(r)$ is the steady state electron temperature before the ECRH switch-on. The vertical solid line is the time moment of the ECRH switch-on. The vertical dashed line is the time delay due to electron ITB.

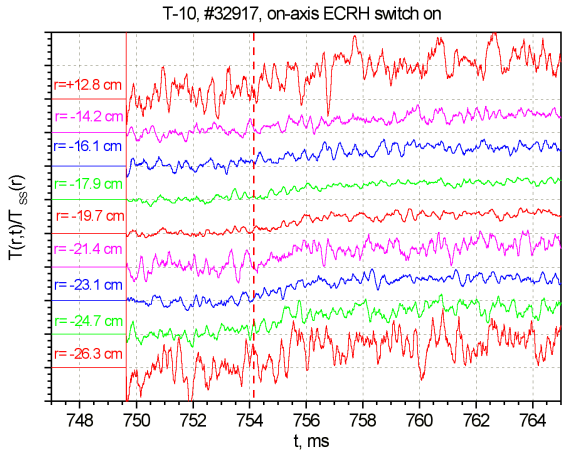

FIG.6. Time evolution of temperature for the peripheral channels 12.8 cm <|r|< 26.3 cm after the on-axis ECRH switch-on with the suppressed saw-tooth oscillations (shot #32917). $T_{SS}(r)$ is the steady state electron temperature before the ECRH switch-on. The vertical solid line is the time moment of the ECRH switch-on. The vertical dashed line is the time delay due to electron ITB.

One can see that the temperature begins to increase in all peripheral channels practically simultaneously. That is, the heat flux propagates from the position of the destroyed electron ITB ($|r|$~10÷12 cm) to the plasma edge ($|r|$~26÷30 cm) practically instantly. In this case one can say that there is a jump of the heat flux through the all plasma radius. The heat flux appears at the plasma periphery (shot #32917) with the time delay twice greater then in the shot #32916. It points out the dependence of time delay on the value of the input ECRH power. In the shot #32917 the power is twice less than in the #32916 (P_{EC}~300 kW). Therefore the more time is necessary for the electron temperature gradient to achieve the critical value.

The existence of the electron ITB in the region ρ~0.28÷0.35 (paragraph 3) explains the electron temperature evolution with the suppressed saw-tooth oscillations (see *FIG.5-FIG.6*). When the gradient of the electron temperature ∇T exceeds some critical value (the relative increase of the electron temperature in the plasma centre is $T(r,t)/T_{SS}(r)$~1.65÷1.75, see *FIG.1*) the electron ITB is destroyed and cannot keep the heat in the heating region. In this moment the heat flux appears at the periphery practically instantly.

FIG.7 shows the time evolution of the electron temperature for the peripheral channels after the additional switch-on of off-axis ECRH in the regime with the suppressed saw-tooth oscillations (the third gyrotron 140 GHz, shot #32912).

FIG.8 shows the time evolution of the electron temperature for the peripheral channels after the switch-off of the one of three off-axis gyrotrons which its suppress the saw-tooth oscillations (the third gyrotron 140 GHz, shot #32912).

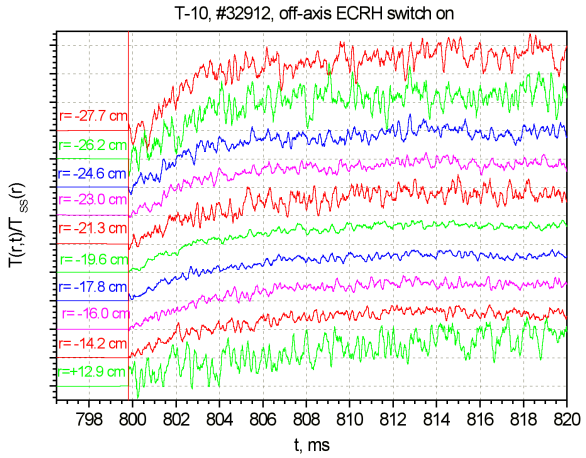

FIG.7. The time evolution of the temperature for the peripheral channels 12.9 cm <|r|< 27.7 cm after the off-axis ECRH switch-on with the suppressed saw-tooth oscillations (the third gyrotron 140 GHz, shot #32912). The vertical line is the time moment of the ECRH switch-on.

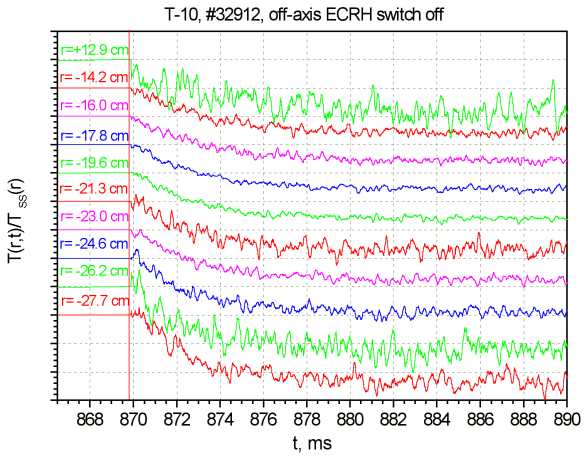

FIG.8. The time evolution of the temperature for the peripheral channels 12.9 cm <|r|< 27.7 cm after the off-axis ECRH switch-off with the suppressed saw-tooth oscillations (the third gyrotron 140 GHz, shot #32912). The vertical line is the time moment of the ECRH switch-off.

One can see from *FIG.7* and *FIG.8* that temperature outside the electron ITB changes practically simultaneously at plasma periphery after the off-axis ECRH switch-on/off. It means that the heat flux spreads from the ECRH region to the periphery practically instantly (with the time less than 0.5 ms). The noises in experimental data do not allow us to distinguish the finite value of velocity of the heat wave propagation during this time scale.

In transport simulations, which deal with the millisecond time scale, fast change of the heat flux (the microsecond time scale) looks like a jump. That is, this process is characterized by the non-diffusive behavior. Probably fast efflux can be due to development of the MHD instabilities driven by the pressure gradient. It was shown [19] that in such a system fast avalanche-like transport is possible in addition to slow diffusive transport.

5. The critical gradient of the electron temperature at plasma periphery

Now let us consider the important peculiarity of the transient process after the off-axis ECRH switch-on/off (the third gyrotron 140 GHz) with the suppressed saw-tooth oscillations. *FIG.5-FIG.8* show that after the off-axis ECRH switch-on/off the electron temperature at the plasma periphery 12 cm <|r|< 27 cm evolves in such way that the relative gradient of the electron temperature remains almost fixed $\nabla T/T \approx const$.

FIG.9 shows few time slices of the electron temperature profiles $T(r,t)$ after the on-axis ECRH switch-on with the suppressed saw-tooth oscillations (shot #32916). One can see that the relative change of electron temperature at the plasma periphery 12 cm <|r|< 27 cm is the same during the time interval $\Delta t \approx 2.0 \div 10$ ms (the experimental curves are parallel one to another).

FIG.10 shows few time slices of the electron temperature profiles $T(r,t)$ after the off-axis ECRH switch-off with the suppressed saw-tooth oscillations (shot #32916). Analogously to the previous case the relative temperature gradient remains fixed at the plasma periphery 12 cm <|r|< 27 cm during time interval $\Delta t \approx 0.5 \div 5$ ms.

So experimental the results (see *FIG.9-FIG.10*) confirm the fact that the relative gradient of the electron temperature at the plasma periphery does not change after ECRH switch-on/off in the suppressed saw-tooth discharges ($\nabla T/T \approx const$).

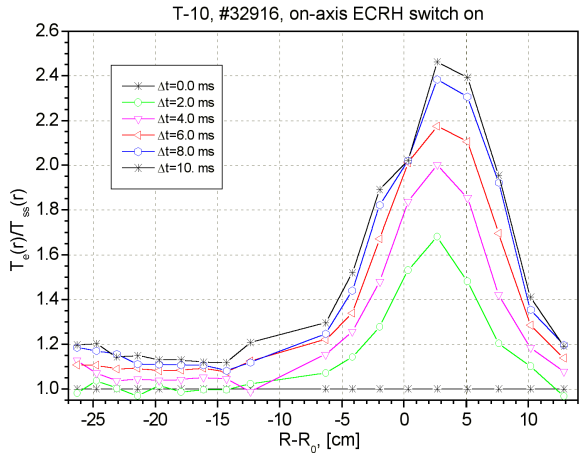

FIG.9. The electron temperature profiles T(r,t) for some time instants after the on-axis ECRH switch-on with the suppressed saw-tooth oscillations (shot #32916, Δt is the time instants after the ECRH switch-on).

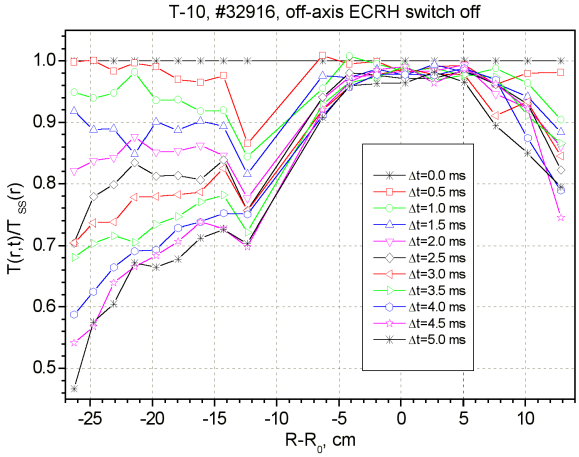

FIG.10. The electron temperature profiles T(r,t) for some time instants after the off-axis ECRH switch-off with the suppressed saw-tooth oscillations (shot #32916, Δt is the time instants after the ECRH switch-off).

Such an evolution of the electron temperature can be explained by the following way. The critical profile of the relative temperature gradient $\nabla T_{cr}/T_{cr}$ is formed at the plasma periphery after the off-axis ECRH switch-on. Therefore when the electron ITB is destroyed or when the auxiliary off-axis ECRH is switched on/off the electron temperature evolves concerning the ration $\nabla T/T \approx \nabla T_{cr}/T_{cr}$.

In papers [19-20] the mathematical model for the description of the ballistic transport process ("sand-pile paradigm") was suggested. It is assumed that under certain conditions the transport system can be characterized by the critical pressure gradient that is any pressure perturbation leads to the instability ("Pressure Gradient Driven Instability"). Auxiliary heating of such a system forms slightly subcritical pressure profile. In case of further input power increase the critical pressure gradient is achieved locally in the heating region. As a result the heat flux spreads very quickly from the heating region to the periphery as an avalanche. This transient process evolves with the MHD time scale. That is practically instantly in comparison with the diffusive process.

Therefore to describe the electron heat transport in tokamak plasma after the ECRH switch-on/off three different physical processes should be taken into account: a) the transient process of plasma heating inside the region bounded by the temporal electron ITB; b) the electron ITB destruction accompanied by the heat efflux to the plasma periphery during the hundreds of microseconds; c) the consequent diffusive evolution of the electron temperature profile with the conservation of the relative temperature gradient $\nabla T/T$.

6. Conclusions

1) In the regimes with the suppressed saw-tooth oscillations (by means of the off-axis ECRH) the electron ITB is formed around the resonance surface q~3/2 (ρ~0.28÷0.35). This ITB explains the delay of the temperature increase at the peripheral channels after the on-axis ECRH switch-on.
2) When the electron temperature gradient in the plasma center exceeds some critical value after the on-axis ECR heating then the ITB is destroyed and the heat flux spreads from the plasma center to periphery "practically instantly".

3) The jump of the heat flux explains the simultaneous change of the electron temperature at the plasma periphery after the off-axis ECRH switch-on/off.
4) The gradient of the electron temperature close to the critical one $\nabla T_{cr}/T_{cr}$ forms outside of the heating region after the off-axis ECRH switch-on.
5) Both after the ITB destruction and after the off-axis ECRH switch-on/off the electron temperature changes in such a way that the relative gradient of the temperature remains fixed ($\nabla T/T \approx \nabla T_{cr}/T_{cr}$).
6) Therefore to describe the electron heat transport in tokamak plasma after the ECRH switch-on/off three different physical processes should be taken into account: a) the transient process of plasma heating inside the region bounded by the temporal electron ITB; b) the electron ITB destruction accompanied by the heat efflux to the plasma periphery during the hundreds of microseconds; c) the consequent diffusive evolution of the temperature profile with the conservation of the relative temperature gradient $\nabla T/T$.

This work was supported by Nuclear Science and Technology Department of Minatom RF; RFBR: №1608.2003.2, №04-02-17562; NWO-RFBR: №047.016.015; INTAS: №2001-2056.

References

[1] K.A. Razumova, V.F. Andreev, A.A. Boshchegovskii, V.V. Chistyakov et al. Plasma Phys. Control. Fusion **45** (2003) 1247-1260.
[2] K.A. Razumova, V.F. Andreev, A.A. Boshchegovskii, Yu.N. Dnestrovskij et al, T-10 team, G.M.D. Hogeweij, R.J.E. Jaspers, E.Min and TEXTOR team. Proc. 30th EPS Conference Control. Fusion and Plasma Phys. 2003, St. Petersburg, Russia (2003), ECA, Vol.27A, P-3.148.
[3] K.A. Razumova, V.F. Andreev, A.J.H. Donne, G.M.D. Hogeweij et al, T-10 team and TEXTOR team. Nuclear Fusion, 2004, **44**, N10, 1067.
[4] G.M.D. Hogeweij, V.F. Andreev, M.R. de Baar, I.Bel'bas et al and TEXTOR team. Proc. 31th EPS Conference on Plasma Phys. London. 2004. ECA Vol.28B, P-1.119 (2004).
[5] Goldston R et al 1987 Plasma Phys. Control. Nucl. Fusion Res. (Proc. 11th IAEA Conf., Kyoto, 1986) **3** 75
[6] Wagner F et al 1986 Phys. Rev. Lett. **56** 2187
[7] Dnestrovskij Yu N and Pereversev G V 1988 Plasma Phys. Control. Fusion **30** 47
[8] Taylor G et al 1989 Nucl. Fusion **29** 3
[9] Suttrop W et al 1997 Plasma Phys. Control. Fusion **39** 2051
[10] Gohil P et al 1998 Nucl. Fusion **38** 425
[11] Horton L D et al 1999 Plasma Phys. Control. Fusion **41** B329
[12] Weiland J et al 1989 Nucl. Fusion **29** 1810
[13] Ryter F et al 2001 Phys. Rev. Lett. **86** 2325, 5498
[14] Jacchia A et al 2002 Nucl. Fusion **42** 1116
[15] Hoang G T et al 2001 Phys. Rev. Lett. **87** 1251
[16] Dnestrovskij Yu N et al. Plasma Phys. Reports 2004 **30** N°1 1-8.
[17] V.F. Andreev, Yu.N. Dnestrovskij, K.A. Razumova, A.V. Sushkov. Plasma Physics Reports, 2002, **28**, No.5, 367-381.
[18] V.F. Andreev, Yu.N. Dnestrovskij, M.V. Ossipenko, K.A. Razumova and A.V. Sushkov. Plasma Phys. Control. Fusion **46** (2004) 319-335.
[19] B.A. Carreras et al 1996 Plasma Phys. Reports **22** N9 819.
[20] T.K. March, S.C. Chapman et al. Physics of Plasmas. 2004. **11**. N°2. 659.